Relationship between the Auger line shape and the electronic properties of graphite

J. E. Houston, J. W. Rogers, Jr., and R. R. Rye

Sandia National Laboratories, Albuquerque, New Mexico 87185

F. L. Hutson and D. E. Ramaker

Chemistry Department, George Washington University, Washington, D.C. 20052

The experimental carbon Auger line shape for graphite has been obtained, corrected for the effects of the secondary-electron background and extrinsic losses, and placed on an absolute energy scale through the use of photoelectron measurements. The resulting line shape is compared to a model which consists of the self-convolution of the graphite one-electron density of states including atomic values for the symmetry-determined Auger matrix elements. A poor comparison results from this simple model which is considerably improved by the inclusion of dynamic initial-state screening effects. Further improvement results from accounting for final-state hole-hole interactions. The final state is characterized by effective hole-hole interaction energies of 2.2 eV corresponding to two holes in the σ band, 1.5 eV for one hole in the σ and one in the π band, and 0.6 eV for both holes in the π band. The remaining discrepancies in our model comparison are suggested to be due to a plasmon emission intrinsically coupled to the Auger final state.

I. INTRODUCTION

The use of detailed Auger spectral line-shape analysis to obtain local electronic structure information has had increased emphasis over the past few years, as is evident from the number of recent review articles devoted to this subject.[1-20] This interest stems from the local nature of the Auger process which has as its initial state a missing core electron. For core-valence-valence Auger transitions, the core-hole state captures a valence electron and transfers its excess energy to the ejection of a second valence electron, the measured Auger electron. The kinetic energy (E_{kin}) of the ejected Auger electron can be approximated,[8,9] by the expression

$$E_{kin} = I_c - I_j - I_k - U_{eff} , \qquad (1)$$

where the I's are the one-electron binding energies of the core (c) and valence (j,k) states involved, and U_{eff} takes into account the interaction between the two final-state holes. Equation (1), of course, refers to a single Auger transition while the Auger spectrum is composed of all possible I_j, I_k combinations. This procedure amounts to taking the self-convolution of the set of valence states I_j or I_k, in other words, to a self-convolution of the density of states (DOS). The local nature of this process stems from the limited spatial extent of the core wave function which ensures that the Auger process probes the valence electron density over the same spatial extent. The implications of this local sensitivity with respect to molecules have been developed in a recent review.[10]

The C(KVV) line shape of graphite (the notation KVV indicates that the core hole is in the K level and both final-state holes are in valence levels) has been the subject of considerable recent study.[21-26] Although much of this attention has been in the context of studying the more novel graphite intercalation compounds,[21,22,27-29] the

graphite Auger spectrum is itself of interest since it represents the infinite limit of the fused ring series: benzene, naphthalene, phenanthrene, etc. In this role the C(KVV) line shape of graphite is unique among the ring aromatic Auger line shapes because the two final-state holes resulting from the Auger process have a chance to delocalize over a much larger volume than would be permitted by the finite size of the molecules.[10] Thus, it is possible that final-state hole-hole correlation effects may be negligible if the holes actually are able to delocalize. In addition, graphite is a model system for studying initial-state, core-hole screening effects in aromatic systems. Previous theoretical calculations have indicated that core-hole screening significantly alters the shape and magnitude of the measured π DOS,[26,30] but the effects of these changes in the graphite Auger line shape have not been examined.

The first attempt at obtaining an accurate C(KVV) line shape for graphite was reported by Smith and Levenson.[23] They utilized a data-reduction procedure which has become almost the standard treatment of Auger data[31] in order to obtain detailed electronic information. The data were taken in the derivative mode and numerically integrated. A background was removed in a manner developed by Sickafus,[32-34] and the resulting Auger line shape was loss deconvoluted utilizing a 263 eV electron elastic peak and attendant loss spectrum.

An attempt at quantitatively interpreting the C(KVV) line shape for graphite reported by Smith and Levenson[23] has recently been reported by Murday et al.[21] They deduced the one-electron partial DOS ($\sigma_s, \sigma_p, \pi_p$) for graphite from x-ray-emission spectra (XES), x-ray-photoemission spectra (XPS), and an assumed electron configuration of $sp^2\pi$. The Auger line shape was then produced from a fold of these one-electron partial DOS assuming noninteracting final-state holes and no screening effects. However, an error (to be discussed later) in their

self-fold makes the agreement with Smith and Levenson fortuitous.

We have obtained graphite C(KVV) spectra which show significant differences from that reported by Smith and Levenson[23] and demonstrate that these differences are due to an improper loss deconvolution of their experimental data. This improper data handling resulted in incorrect assumptions in the subsequent theoretical analysis of Murday et al.[21]

Our C(KVV) line shape for graphite was corrected for both the effects of the secondary-electron background and the extrinsic losses suffered by the Auger electrons in leaving the solid. Extrinsic losses are those external to the Auger process such as those that result from an electron moving through a solid. In contrast, intrinsic losses are associated with the Auger transition. The raw Auger data were taken in two separate laboratories and on three distinct types of electron-energy analyzers, and data-reduction procedures were applied independently in each case. The absolute energy scale for the Auger line has been established by utilizing the valence, core level, and Auger features available concurrently in the graphite XPS. The resulting line shape is compared to a model which consists of the self-convolution of the graphite one-electron density of states including atomic values for the symmetry-determined Auger matrix elements. A poor comparison results from this model which is considerably improved by the inclusion of dynamic screening effects in the initial state. Further improvement in the model results from accounting for the effect of final-state hole-hole interactions through the use of a formalism developed by Cini[35,36] and Sawatzky.[37] From the resulting parametrized-model fit to the experimental line shape, we find effective hole-hole interaction energies of 2.2 eV for two holes in the σ band, 1.5 eV for one hole in the σ and one in the π band, and 0.6 eV for both holes in the π band. Areas of discrepancy remain after the inclusion of corrections for these two effects of many-electron processes and these discrepancies are suggested to be due to a plasmon emission intrinsically coupled to the Auger final state.

II. EXPERIMENTAL

Evaluation of the quality of the data presented here with respect to instrumental and possible sample differences has involved a "round-robin" analysis. The C(KVV) and loss spectra were obtained in the $N(E)$ mode at two different laboratories on three different types of electron-energy analyzers: a narrow-aperture, retarding, partial-hemispherical sector instrument; a medium-aperture, retarding, full-hemispherical, sector instrument; and a retarding, double-pass, cylindrical-mirror analyzer.

Spectra were obtained from the basal plane of single-crystal graphite (SCG), highly oriented pyrolytic graphite (HOPG), and POCO graphite (POCO Graphite Co., Decatur, TX), a machinable amorphous graphite. For the HOPG and SCG samples a layer was peeled off just prior to insertion into the vacuum system and all samples were heated to $\simeq 1200$ K by electron bombardment from the backside. In the particular case of the SCG sample, XPS

analysis yielded no detectable core-level peaks other than C(1s) even after several days in the vacuum system. The medium-aperture, retarding, full-hemispherical, sector analyzer system had an associated x-ray source and a helium lamp in addition to the electron gun. As a result it was possible to obtain in the same scan the x-ray-excited Auger, core level, and valence spectra all calibrated to the graphite Fermi level; and to obtain, without repositioning of the sample, the ultraviolet valence spectrum or the electron-excited Auger spectrum.

III. RESULTS AND ANALYSIS

Figure 1 shows an example of the electron-excited Auger results from the POCO graphite sample prepared in the manner just described taken in the $N(E)$ mode with the narrow-aperture analyzer. Raw data of the type shown in Fig. 1(a) results from the true Auger spectrum as well as contributions from two factors: (1) the spectra reside on the secondary electron background and (2) the outgoing Auger electrons lose energy in traveling through the near-surface region of the sample. The second of these effects is evident in the structure and the featureless tail on the low kinetic energy side of the spectrum. To obtain a more representative measure of the undistorted Auger line shape, these effects must be removed from the raw data. Houston[31] has treated these line-shape distor-
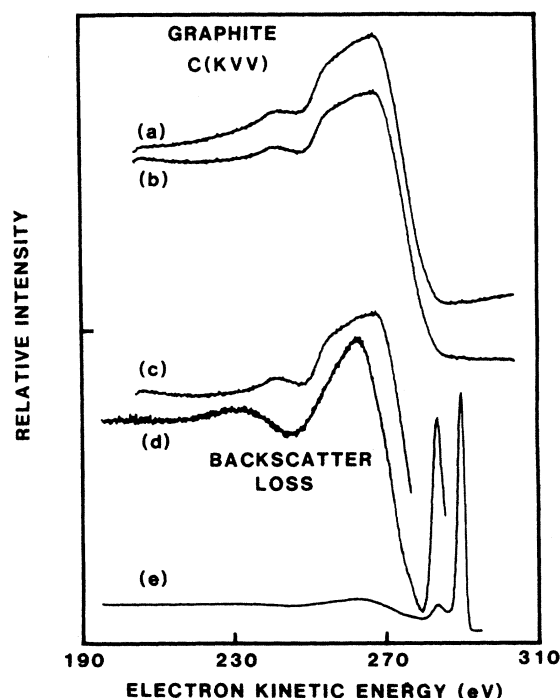

FIG. 1. (a) The raw data for the electron-excited C(KVV) Auger region of POCO graphite taken in the $N(E)$ mode. (b) The raw Auger data corrected for a linear secondary-electron background. (e) The electron backscatter spectrum of POCO graphite using 290 eV incident electrons. Curves (d) and (c) show a comparison of the low-energy loss structure of (e), on an expanded vertical scale, and the background corrected Auger data of (b), respectively.

tions in detail in a recent publication in which data simi-lar to that in Fig. 1(a) was used as an example. Various analytic functions are described for direct background subtraction[32-34] and the effect of the losses is removed by a deconvolution procedure utilizing model loss functions.[19,38]

In applying these procedures, it is assumed that in the absence of the background there exists a "true" Auger line shape covering a limited energy range, i.e., an Auger line, which when convoluted by the proper loss function for the material under study yields the background-corrected raw data. The loss function is the line shape that would be measured if one had a monoenergetic, internal source of Auger electrons. Such a source is, of course, not available and one must use approximate loss functions to ac-complish the line-shape correction. An approximate loss function that is easily obtained and often used is that of the elastic and near-elastic electron backscatter spectrum resulting from a monoenergetic electron beam incident on the sample surface at an energy near that of the Auger feature. Although this model loss function may in some cases not be adequate, we justify its use here because of the similarity in shape that we find between the back-scatter spectrum and the XPS core-level spectrum for graphite—the photoelectron being a much better approxi-mation to an Auger electron than a backscatter electron. The principal remaining difficulty in using the back-scatter approximation for the model loss function is that we have no valid model for the "intrinsic" losses associat-ed with the Auger process and these, if appreciable, remain in the deconvoluted Auger line shape. This point will turn out to be important in the ensuing discussion.

The backscatter approximation to the loss function is shown in Fig. 1(e) taken at an incident electron energy of 290 eV. One can see from this data the two graphite characteristic losses (usually described as "plasmon" losses) at loss energies of approximately 7 and 27 eV; these appear very similar to the previously published[39] loss features associated with the XPS C(1s) line. It should be noted that the instrument response of the electron-energy analyzer used to obtain the data of Fig. 1 is given by the shape of the elastic portion of this spec-trum.

In subtracting the proper background from the raw Auger data one normally utilizes low-order polynomials for weakly varying backgrounds like that shown in Fig. 1(a). For our present purposes only a slight linear back-ground correction was necessary and the result of such a background subtraction is shown in Fig. 1(b). The criteria for a properly corrected background are the following: (1) that the region of the corrected spectrum with energies above the Auger threshold [> 280 eV in Fig. 1(b)] should be flat and at the zero baseline and (2) that the featureless region below the structure in the background-corrected data [< 230 eV in Fig. 1(b)] should accurately match in shape the corresponding region in the loss function. The shape similarity in this region is evident from the compar-ison shown in Figs. 1(c) and 1(d). If these criteria are not met then one of the basic assumptions concerning the deconvolution procedure is not fulfilled and a proper deconvolution cannot be made.

Since the true loss function is not available, one other assumption is necessary for proper loss correction by deconvolution. We must assume that the general shape of the model function is the same as the true loss function, the only possible difference being the relative intensities of the loss features with respect to that of the elastic peak. In the commonly used procedure,[31] the losses are stripped away from the elastic peak, the elastic peak is normalized to a unit area and then the losses are replaced, scaled by an adjustable parameter. The deconvolution is then per-formed interactively adjusting the scaling parameter to achieve a flat and zero baseline behavior in the low-energy region beyond the characteristic features.

The result of this procedure for the data of Figs. 1(b) and 1(e) is shown in Fig. 2. Careful attention to the cri-teria just described results in corrected spectra which are very reproducible, probably to within ±20%, in the low-energy region of the Auger line where the deconvolution procedure is most susceptible to error. Any distortions between the results given in Fig. 2 and the "true" Auger spectrum are minimal in the threshold region and progres-sively increase through the low-energy tail.

Significant angular-dependent line-shape variations have been found in the main body of the Auger spectrum for HOPG and SCG samples.[40] In order to better approx-imate the graphite spectrum in terms of one-electron models which are angle integrated in nature, we have chosen to use the POCO graphite results of Fig. 1 in our subsequent analyses.

The Fermi level noted by the FL line in Fig. 2 was ac-curately established in a separate experiment in which the x-ray excited Auger, the core level, and valence spectra were obtained simultaneously. The Fermi level expressed on a E_{kin} scale is simply the measured C(1s) binding ener-gy of 284.6 eV. An example of this data is shown in Fig. 3. These results permit an accurate calibration of the Auger kinetic energy with respect to the Fermi energy.

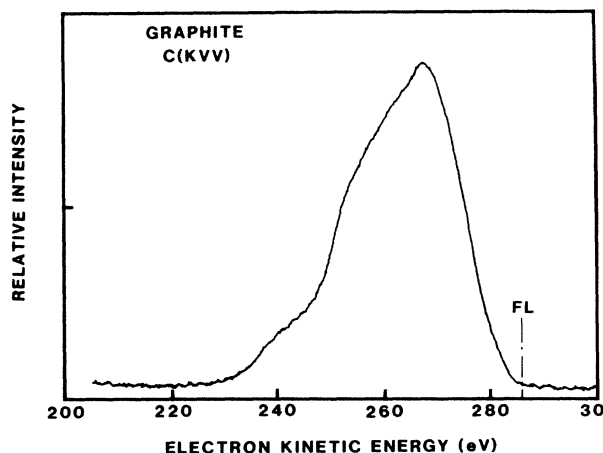It should be noted with respect to the corrected Auger

FIG. 2. The C(KVV) line shape for POCO graphite corrected for secondary-electron background and the effects of extrinsic loss processes by loss deconvolution. The Fermi level (FL) in this kinetic energy scale is located at the C(1s) binding energy of 284.6 eV.
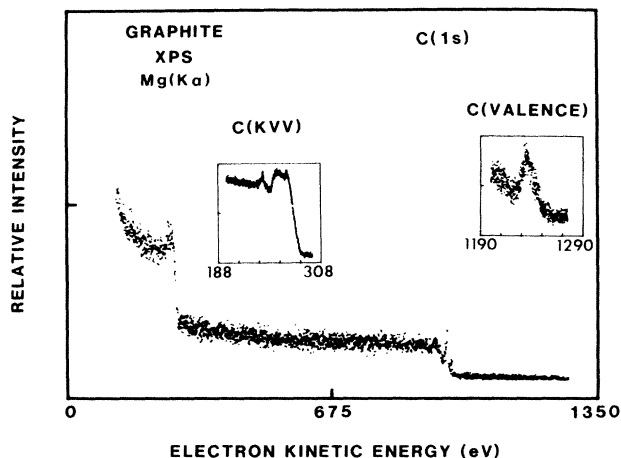
FIG. 3. Broad scan high-resolution XPS for POCO graphite showing the valence and Auger regions as well as the C(1s) line. The insets show expanded views of the valence and Auger regions.

line shape of Fig. 2 that similarly obtained results reported earlier by Smith and Levenson[23] show a considerably narrower line with no apparent low-energy structure. However, the background-corrected raw data and elastic and near-elastic backscatter spectra shown in the Smith and Levenson paper (Figs. 1 and 2 of Ref. 23) do not satisfy the shape criterion in the low-energy tail region as we have just discussed. The result of this mismatch is that the deconvolution forces the corrected spectrum to go negative in the low-energy region. Using our spectra in Figs. 1(b) and 1(e), the deconvoluted results of Smith and Levenson can only be approximately obtained by a serious distortion of the deconvolution procedure. Apparently, Smith and Levenson truncated their corrected spectrum at the point at which it went negative (due to improper removal of the featureless tail) giving the impression of a narrower line with no intensity in the low-energy region.

Because of the possibility of distorted line shapes similar to that experienced by Smith and Levenson resulting from the data-reduction procedures, we have taken particular care to evaluate the reliability of the experimental data and the data-manipulation procedures presented here. We have obtained corrected Auger line-shape data independently from three different graphite samples, three different spectrometers, and at two separate laboratories. This procedure resulted in very similar line shapes for similarly prepared POCO graphite samples. The relative intensity of the feature in the low-energy region at about 245 eV (which is the most sensitive to the data-manipulation techniques for all samples) was found to vary in our experiments by about 20%, but the feature was always present. With this relative accuracy in mind, in the remainder of this paper we will attempt to clarify the origins of the graphite line shape.

IV. DISCUSSION

In attempting to characterize the Auger line shape for graphite in terms of its known electronic properties it is

helpful to begin as simply as possible and allow the disagreement between the model characterization and the experimental result to guide further sophistication. For this approach, the simplest model involves the one-electron approximation with the inclusion of the Auger matrix elements based on similar transitions in rare-gas atoms. We begin the present discussion with such a comparison and continue by using the nature of the disagreement as a guide to the inclusion of "many-electron" effects such as initial-state screening, shake phenomena, hole-hole correlation, and dynamic final-state screening.

A. One-electron approach

Murday et al.[21] have deduced from experimental data the graphite partial density of states (PDOS) components: π_p, σ_p, and σ_s. The p electrons contribute to both the π and σ bands. The σ_s PDOS was obtained from the XPS valence band[39] where the intensity is primarily determined by s symmetry [i.e., XPS intensity is $\sigma_s + \frac{1}{32}(\sigma_p + \pi_p)$].[21] The σ_p and π_p PDOS was obtained from angular-dependent XES data:[41] the σ_p PDOS was obtained from data at 80° take-off angle and the π_p from 5° data. The relative areas of the individual PDOS were normalized to provide a $\sigma_s \sigma_p^2 \pi$ configuration. This total empirical DOS has been found to agree reasonably well with theoretical calculations[42-44] except for the overall bandwidth. Murday et al.,[21] forced the bandwidths to agree by arbitrarily truncating the PDOS.

Such truncation is reasonable since the empirical procedures for determining PDOS all involve experimental results from excitation or deexcitation techniques that are not in themselves one electron in nature. These techniques invariably show bands that are broader than expected theoretically, presumably due to the effects of intrinsic processes, and truncation has become a common procedure to correct for such effects.[21,39,45] However, since we are trying to model a many-electron process by manipulating the results of other many-electron processes, it seems more reasonable to utilize the data itself rather than perform an arbitrary truncation. Therefore, we show the results of the Murday et al. procedure without data truncation as the solid lines in Fig. 4. It is clear that this truncation produces only a very small effect and we show later that the effect is relatively even smaller in our convolution model. Figure 4(a) contains the σ_s and σ_p components, scaled for a $\sigma_s \sigma_p^2 \pi$ electron configuration, of the PDOS as obtained from the XES and XPS data; Fig. 4(b) contains the σ and π PDOS ($\sigma = \sigma_s + \sigma_p$); and Fig. 4(c) is the total DOS ($\sigma + \pi$). The dotted section of Fig. 4(c) illustrates the truncated results published by Murday et al.[21] The XES and XPS leading to the PDOS in Fig. 4 were originally referenced to the graphite Fermi energy and the energy scale shown in Fig. 4 was obtained by adding the graphite C(1s) binding energy (284.6 eV) to this Fermi energy. Thus, both the empirical PDOS data and the experimental Auger line shape of Fig. 2 are placed on a common absolute energy scale and the subsequent modeling will be done without altering these energy scales.

As mentioned earlier, the model Auger line shape $A(E)$ in the one-electron approximation can be generated by
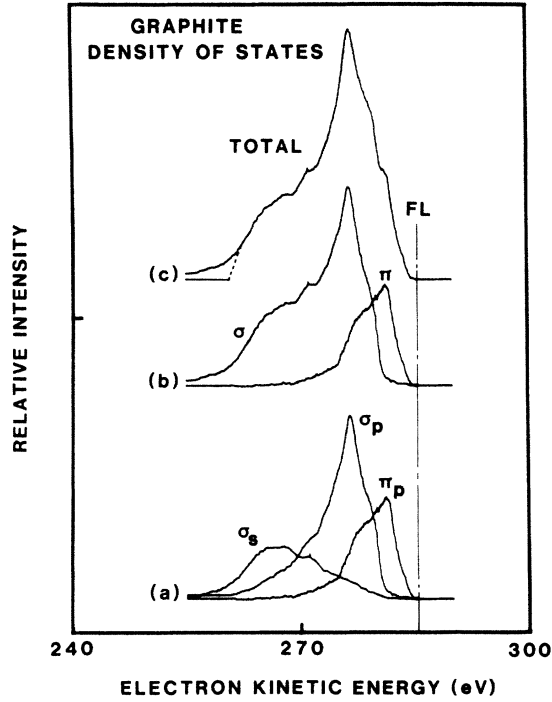
FIG. 4. (a) The empirical graphite partial density-of-states (PDOS) components obtained following the procedure of Murday et al. (Ref. 21). (b) The two-band PDOS where the σ band is formed by summing the σ_s and σ_p PDOS. (c) The total DOS formed by summing the PDOS of (a). The vertical line marked FL shows the position of the Fermi level and the curves have all been shifted upward in energy by the C(1s) binding energy of 284.6 eV. The dotted portion of (c) shows the truncated total DOS as given by Murday et al. (Ref. 21).
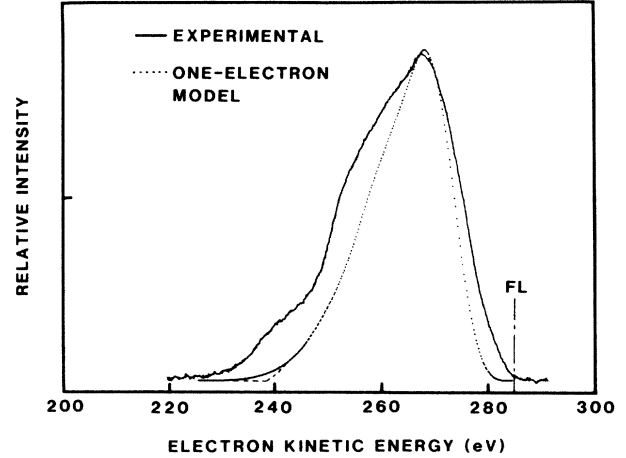

FIG. 5. A comparison of the experimental Auger line shape for POCO graphite (solid curve) with the one-electron model calculated as the self-convolution of the PDOS from Fig. 4(a), modulated by the symmetry-dependent Auger matrix elements. The vertical line marked FL shows the position of the Fermi level. The dashed portion of the model curve shows the effect of using the truncated total DOS of Murday et al. (Ref. 21) from Fig. 4(c).

self-folding the DOS. In terms of the three PDOS components shown in Fig. 4(a), this procedure results in the expression,[8]

$$A(E) = P_{kss}\sigma_s * \sigma_s + 2P_{ksp}(\sigma_s * \sigma_p + \sigma_s * \pi_p)$$
$$+ P_{kpp}(\sigma_p * \sigma_p + 2\sigma_p * \pi_p + \pi_p * \pi_p) \quad (2)$$

where the $\sigma_s * \sigma_s$, etc., terms indicate a fold of the PDOS components,

$$\sigma_s * \sigma_s = \int \sigma_s(E)\sigma_s(E - \epsilon)d\epsilon , \quad (3)$$

and the $P_{kll'}$ factors are atomic Auger matrix elements normalized per electron. These atomic matrix elements are assumed to be the same as those determined from both experiment and theory for atomic neon:[8,46]

$$A_{kss}/A_{kpp} = 0.089, \quad A_{ksp}/A_{kpp} = 0.034 .$$

A plot of the relative contributions, $A_{kll'}$, as a function of Z, the nuclear charge, reveals that the ratios ($ll' = ss$, sp, and pp), are remarkably constant from atom to atom.[8] From the expressions,

$$\frac{A_{kss}}{A_{kpp}} = \frac{4P_{kss}}{36P_{kpp}} \text{ and } \frac{A_{ksp}}{A_{kpp}} = \frac{24P_{ksp}}{36P_{kpp}} , \quad (4)$$

the relative atomic Auger matrix elements per electron can be obtained; $P_{kss}:P_{ksp}:P_{kpp} = 0.8:0.5:1.0$. Although these same matrix elements were utilized by Murday et al.,[21] the factor of 2 in front of the $\sigma_p * \pi_p$ term in Eq. (2) was inadvertently omitted in their work. Thus, the $\sigma_p * \pi_p$ intensity in their Fig. 2 is a factor of 2 too small.

We can now use Eq. (2) and the nontruncated PDOS functions of Fig. 4(a) to generate the one-electron model function for the Auger line shape which is shown as the dotted curve in Fig. 5. The dashed partion shows the effect of truncating the PDOS (Ref. 21) and, as we indicated earlier, truncation has a negligible affect on our model line shape. The experimental result from Fig. 2 is shown as the solid curve and it is apparent from this comparison that the one-electron model of the Auger line shape significantly differs from the experimental result in several respects regardless of whether a truncated or nontruncated PDOS is used. The model line shape is appreciably narrower than the experimental result with intensity missing in both the threshold region near 280 eV and in the area below the principal maximum at about 260 eV. Thus, it is clear that processes other than those encompassed by the one-electron model play a significant role in determining the graphite Auger line shape.

B. Many-electron effects

The one-electron approximation assumes that the Auger transition begins with an excited core state (core hole) and ends with two holes in valence levels along with an Auger electron in the continuum. During this entire process, the valence electronic levels are considered to be frozen in their ground-state configurations, which would imply that the electrons of the system are noninteracting. Of course, if this were true there would be no Auger tran-

sition, so it is obvious that the approximation is going to break down and the only question is, "How does this break down manifest itself in the Auger line shape and to what relative magnitude?" We will structure our discussion of many-electron effects as if they were separable in their contribution to the Auger line shape which is somewhat artificial since the effects are all part of the same phenomenon. The various effects will be discussed according to their contributions to the different regions of the spectrum including those which principally affect the intensity of the self-fold components, those which give rise to intensity above threshold, and those which contribute to low-energy intensity.

1. Static initial-state screening

The static screening response of the valence electrons to the presence of the core hole in the Auger initial state[30,47] has been shown to contribute to the intensity of the various self-fold components. The term "static" differentiates this aspect of the screening response from the dynamic shake phenomena that will be discussed below. This distinction has been discussed recently by Sawatzky[48] with respect to core-hole creation in photoelectron spectroscopy. If one slowly, or adiabatically, creates a core hole in a solid-state atom the electronic states will adjust themselves in an attempt to lower the energy of the core-hole state. The static screening response amounts to the situation where the core-hole creation results in the fully relaxed state with the electronic states polarized as if they were responding to the presence of the $Z + 1$ impurity state.

Static screening has been discussed for Auger transitions by Ramaker and co-workers,[26,47,49] and by Jennison[30] and can be illustrated through the use of the final-state rule (FS rule). The FS rule indicates that the total intensities of the various symmetry components making up the Auger line shape (ss, sp, etc.) are determined by their electronic configuration appropriate to the statically screened initial-state core hole, while the shape of each contribution is determined by the appropriate final-state DOS.[47] If we further assume that the final-state holes are noninteracting, then according to the FS rule the ground-state DOS can be substituted for the final DOS as was done by Murday et al.[21]

The statically screened, initial-state configuration has been determined recently from a parametrized 109 atom cluster LCAO-MO calculation by Dunlap, et al.[26] under the assumption that only the unfilled π band makes a significant contribution. It was found that the local electron density in the π band increased by 0.55 electrons to a $\sigma_s \sigma_p^2 \pi^{1.55}$ configuration. However, recent calculations by Binkley[50] on benzene and pyridine suggest that the screening response of the other components of the valence band are also important. Benzene with a core hole at one carbon site and the ground-state electron density at the nitrogen site in pyridine give essentially the same result indicating that the π screening charge is increased by about 0.54 (in agreement with Dunlap et al.[26]) and that the σ_p and σ_s states pick up about 0.23 and 0.52 electrons, respectively, as a result of static, initial-state screening.
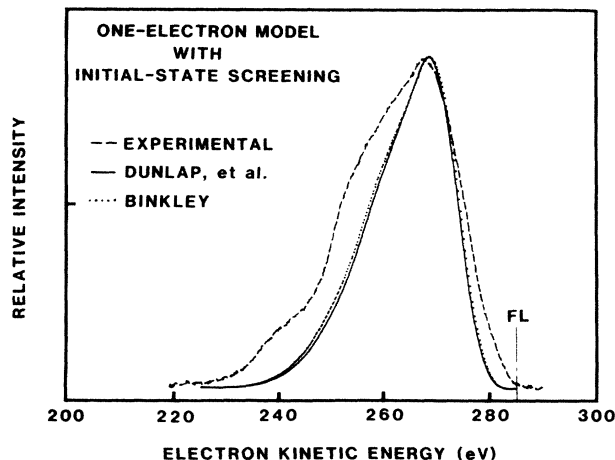

FIG. 6. A comparison of the effect on the Auger model of static initial-state screening using the partial band occupancy values of Dunlap et al. (solid curve) (Ref. 26), which assumes that only the π band is involved in the screening, and the occupancy values of Binkley (Ref. 50), which includes the contribution from all bands (dotted curve). The experimental spectrum from Fig. 2 is shown as the dashed curve.

These variations in the initial-state electron occupation result in only minor changes in the model Auger line shape as illustrated in Fig. 6. Here, the solid curve includes only the π-level screening of Dunlap et al.[26] and the dotted curve includes screening from all the bands using the Binkley[50] parameters. The level of agreement with the experimental spectrum is only slightly changed in either case.

The model line shapes in Fig. 6 were obtained utilizing the FS rule as stated above, which is known to break down within a few eV of the Fermi level[21] suggesting that the difference near the top of the line shape between the model and experiment might result from this breakdown. However, our model line shape was obtained by folding empirically determined PDOS from the XES, and if the FS rule is seriously breaking down for the Auger line shape, it would similarly break down for the XES line shape. Thus nonorthogonality effects between the initial-state and final-state near the Fermi level have been included implicitly in the model. In addition, the calculations by Dunlap et al.[26] indicate that these nonorthogonality effects are relatively small for graphite.

2. Dynamic initial-state screening

As shown, static, initial-state screening cannot account for the differences between the model line shape and experiment for the region of the Auger spectrum just below the Fermi level. However, there are several dynamic screening effects involving the initial state which can give rise to structure in this region. For example, the sudden creation of a core hole can lead to shakeup processes which leave the system in a more energetic initial state than a statically screened core hole. If this excited situation remains local to the core-hole site for sufficient time, the Auger transition can utilize electrons in the excited

state and produce intensity at higher energies than expected on the basis of a static screening model.

Shakeup structure of this kind is well known in gas-phase molecules,[51] transition metals,[52] semiconductors, and insulators.[53] Such excited states can readily be produced by electron and off-resonant photon excitation near the core-hole excitation threshold and specific excited states can be produced by resonant photon excitation. Graphite is known to have a prominent resonant excitation structure just above the Fermi level resulting from a core-excitonic state, i.e., an excited state consisting of a conduction-band electron bound to the excited core hole. The existence of this state was established by Mele and Ritsko[54] using electron energy loss spectroscopy with 80 keV incident electrons. In their spectra the core-excitonic state is seen as a sharp level centered at about 1 eV above the Fermi level with a full width at half maximum of about 1.0 eV.

If this core-excitonic state were involved in the subsequent Auger transition, then we would expect to see intensity in the high-energy region of the Auger spectrum in electron-excited results but not in off-resonant, photon-excited measurements. In fact, we find identical line shapes using electron excitation and excitation by $Mg(K\alpha)$ photons (1253.6 eV). Thus, it is apparent that direct excitation into the core-excitonic state does not result in appreciable Auger intensity.

The reason that resonant excitation into the core-excitonic state does not contribute significant Auger intensity is no doubt due to the short-lived existence of an electron in this state. From the lifetime broadening of the $C(1s)$ core state[55] and the core-excitonic state[54] (0.06 and 1.0 eV, respectively), we estimate that the lifetime of the former is about 17 times the latter. Thus, there is only a small probability that this directly populated core-excitonic state would be occupied during the Auger transition.

Van Attekum and Wertheim[56] have shown that the $C(1s)$ XPS spectral line shape of graphite is distorted due to the shakeup of a valence electron into an excitoniclike level near the Fermi level during the core excitation. This process, which we will term a valence-core exciton, differs from the direct excitation in that the resultant Auger initial state would contain two positive holes, one in the core level and one in a valence level, with one electron in the excitonic level. (The direct excitation process has a missing core electron and an electron occupying the excitonic level.) Their analysis suggested a lifetime broadened width for this excited condition of approximately 0.1 eV indicating a lifetime an order of magnitude longer than the directly populated core exciton (1.0 eV) and one approaching that of the core hole (0.06 eV). It is probable that this valence-core exciton does make a contribution to the threshold region of the graphite Auger spectrum. Moreover, since the fluorescent yield for graphite[55] indicates a photon decay lifetime width of only 0.0002 eV, the valence-core exciton is not expected to contribute to the XES.

Inclusion of the valence-core exciton results in significant line-shape changes since it gives rise to intensity in the threshold region just below the Fermi level where in-
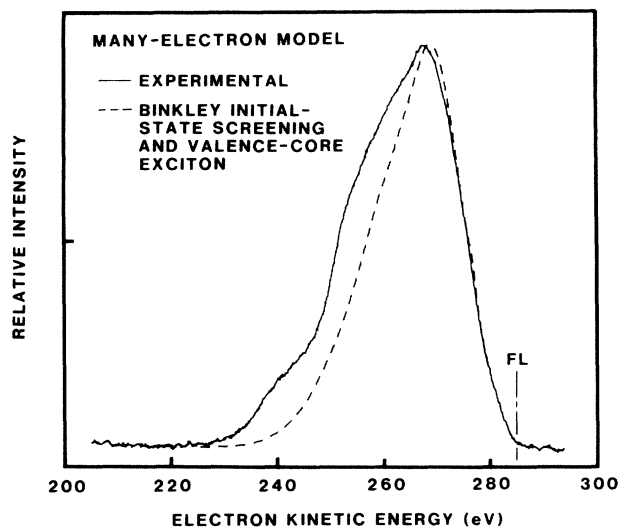

FIG. 7. A comparison of the experimental Auger line shape of POCO graphite (solid) with a model which includes the initial-state occupancy values of Binkley (Ref. 50) and the effect of the valence-core excitonic state located at the Fermi level effectively containing 0.27 electrons (dashed).

tensity is missing in the model spectra in Figs. 5 and 6. This can be seen in Fig. 7 where we have included the electron density arising from shakeup into the valence-core excitonic state as a delta function at the Fermi level and varied its electron occupancy to obtain a "best fit" with the leading edge of the experimental result. We have assumed that the excited electron in the valence-core excitonic state has p symmetry and have used the appropriate Auger matrix elements discussed earlier. The value for the effective electron occupancy in the valence-core excitonic state obtained by this procedure is 0.27 electrons which appears reasonable compared with the intensity in the lower shoulder of the core XPS peak.[56] A full account of the origin and modeling of this feature is given elsewhere.[57]

The additional intensity in the high-energy region of the spectrum shown in Fig. 7 should take two forms: (1) a sharp feature located near the Fermi level resulting from the Auger transition which leaves two holes in the valence-core excitonic state and (2) a broader structure located below the Fermi energy resulting from the transition which places one hole in the valence-core excitonic level and one in the valence band. The fact that the experimental Auger spectrum shows no sharp feature near the Fermi energy simply means that the effective occupancy of the valence-core excitonic state is not sufficient to give rise to a significant probability of it being doubly occupied. Simple statistical arguments suggest that an average effective occupancy of 0.27 electrons in this state would lead to an intensity ratio of about 5% between the Auger feature resulting from both holes in the valence-core excitonic state compared to one hole in this state. Thus, it is not surprising that this feature is not seen above the noise level in the experimental spectrum.

It is interesting to note that in intercalated graphite with a donor intercalant, e.g., alkali metals, the Fermi-

level position increases as some of the normally empty conduction-band states are filled.[26] This process gives rise to an increased occupancy of the core-excitonic Auger initial state and a sharp feature of significant intensity near the Auger threshold. Furthermore, the lifetime of this core-excitonic screening charge is long since it is part of the static screening process and lies below the Fermi level. The intensity of this core-excitonic contribution is found to increase as the square of the intercalant concentration, whereas the intensity of the structure which would correspond to that enhanced in Fig. 7 only increases in a linear fashion.[27] This is to be expected on the basis of the probability of double-hole occupancy of the core-excitonic state relative to single-hole occupancy.

From the comparison of Fig. 7, we can see that dramatic improvement is obtained in the near—Fermi-level portion of the model by including the effect of the dynamic initial-state Auger processes. However, significant discrepancies remain in the area below the principal peak and it is apparent that other many-electron effects must be taken into account.

3. Final-state hole-hole interaction

The Auger transition, being two-electron in nature, causes a unique many-electron effect which significantly distorts the line shape compared to that expected from a one-electron model. The effects of hole-hole interaction on Auger line shapes has been modeled for simple systems by Cini[35,36] and Sawatzky.[37] The holes tend to remain spatially localized after the Auger transition giving rise to a net Coulomb repulsion characterized by the effective energy value U_{eff}. Cini has given the following expression[35,36] for the distortion caused by localization of the Auger final-state holes:

$$A(E) = \frac{N(E)*N(E)}{[1 - U_{eff}I_{NN}(E)]^2 + \pi^2 U_{eff}^2 [N(E)*N(E)]^2}, \quad (5)$$

where $N(E)*N(E)$, the self-fold of the one-electron DOS, $N(E)$, represents the undistorted Auger line shape in the one-electron approximation of Eq. (2), and $I_{NN}(E)$ is the Hilbert transform of $N(E)*N(E)$. The Cini expression was derived from a many-electron calculation on a single filled band.

As was demonstrated by Cini,[36] the effect of the hole-hole interaction is to shift spectral intensity toward the low-energy end of the line shape as the value of U_{eff} is increased. The energy positions of the top and bottom of the spectrum do not change from their one-electron values. As the value of U_{eff} becomes greater than the width of the original valence band, a discrete state can be split off below the main Auger structure. This discrete structure is expected to be much narrower and more intense than that of the main portion of the Auger spectrum.

In attempting to model the effect of the hole-hole interaction in graphite using the Cini expression, we must first address the fact that we are not dealing with a single, filled-band system. In fact, in graphite we have two bands as shown in Fig. 4(b) (the σ and π bands) both of which are half filled. In addition, the atomic-orbital com-

position of the σ band varies with position in the band as shown in Fig. 4(a). To our knowledge, no theoretical expression is presently available corresponding to Eq. (5) for half-filled bands, although Cini and others have discussed the case of a small number of empty states in an otherwise filled band.[58,59] Significantly unfilled bands complicate the situation by introducing an increased screening response in such systems. In the absence of an adequate theoretical treatment for this case, we will assume that the mixing of the empty states in the σ and π bands is small and will only affect the value of U_{eff} in Eq. (5). This assumption seems reasonable since the antibonding portion of the σ band is split off from the bonding portion and we have shown previously that as long as U_{eff} is small relative to this separation, the bonding and antibonding bands do not mix.[60] This assumption may not be valid for the π band, but the excellent agreement between the one-electron model with dynamic initial-state screening effects and the experimental Auger line shape near the Fermi level,[57] indicates that localization effects here are negligible anyway.

A problem with using the Cini expression on a filled degenerate two-band system arises from the possibility that the bands could mix giving rise to cross terms in the distortion expression. Cini has shown formally that the extension of his theory to degenerate orbitals and bands can be solved exactly, but the calculations and results are very complicated.[36] He has suggested that if the solid does not distort the spherical symmetry of the atom significantly, such as in metals, the equations for the different total angular momenta, decouple so that each ^{2s+1}L multiplet component can be treated as an independent band using Eq. (5) with a different U_{eff} parameter for each. Previously, Weightman and Andrews[61,62] analyzed their Auger spectra of transition metals and alloys with this approximation and obtained good agreement with experiment.

The spherical-symmetry approximation is not valid for graphite, or for that matter, for any covalently bonded solid, but we can make a similar approximation utilizing the local D_{3h} planar symmetry around each carbon atom. Utilizing this approximation each ^{2s+1}A multiplet decouples in a manner similar to that used by Ramaker[63] for a molecular-orbital cluster calculation for SiO_2. However, the number of different multiplets and U_{eff} parameters which arise becomes large and the essential physics is difficult to ascertain.

We prefer a more intuitive approach which we believe is valid, since the magnitude of the correlation effects in graphite is certainly much less than in either SiO_2 or in the transition metal alloys.[61,62] We assume that multiplets coming from the individual $\sigma*\sigma$, $\sigma*\pi$, and $\pi*\pi$ folds have a common U_{eff} value, thus reducing the number of parameters to three. Furthermore we assume that the relative separation in energy between the $\sigma*\sigma$, $\sigma*\pi$, and $\pi*\pi$ contributions is large compared to U_{eff}, so that the three contributions can be considered separately. The effect of the Auger matrix elements will be handled by projecting the symmetry components onto the Cini distortion function and multiplying the result by the appropriate matrix-element values. As an example, for the σ band we

first write the Cini distortion function from Eq. (5) as

$$F_{\sigma\sigma} = \frac{1}{(1 - U_{\sigma\sigma}I_{\sigma\sigma})^2 + \pi^2 U_{\sigma\sigma}^2 (N_\sigma * N_\sigma)^2} , \quad (6)$$

where $N_\sigma * N_\sigma$ is the total σ band self-fold

$$N_\sigma * N_\sigma = \sigma_s * \sigma_s + 2\sigma_s * \sigma_p + \sigma_p * \sigma_p . \quad (7)$$

Therefore, the three Cini distorted Auger contributions are given by the expressions

$$A_{\sigma\sigma} = F_{\sigma\sigma}(\sigma_s * \sigma_s P_{kss} + 2\sigma_s * \sigma_p P_{ksp} + \sigma_p * \sigma_p P_{kpp}) , \quad (8)$$

$$A_{\sigma\pi} = 2F_{\sigma\pi}(\sigma_s * \pi_p P_{ksp} + \sigma_p * \pi_p P_{kpp}) , \quad (9)$$

$$A_{\pi\pi} = F_{\pi\pi}\pi_p * \pi_p P_{kpp} , \quad (10)$$

where the P_{kss}, P_{ksp}, and P_{kpp} terms are the relative matrix elements given earlier. We now have just three components with three different values of U_{eff}, and the model line shape is given by

$$A(E) = A_{\sigma\sigma}(E) + A_{\sigma\pi}(E) + A_{\pi\pi}(E) . \quad (11)$$

Using this procedure, we are able to produce the "best-fit" data shown as the dashed curve in Fig. 8. The dotted curves A, B, and C are, respectively, the contributions $A_{\sigma\sigma}$, $A_{\sigma\pi}$, and $A_{\pi\pi}$ from Eqs. (8)–(10), and D is the valence-core exciton contribution.[57] This particular model Auger line shape was obtained with U_{eff} values of 2.2, 1.5, and 0.6 eV for the $\sigma * \sigma$, $\sigma * \pi$, and $\pi * \pi$ self-folds, respectively. The near-zero value of U_{eff} for the $\pi * \pi$ self-fold is consistent with previous data for benzene[10] where U_{eff} for the π transitions reflects delocalization to the dimensions of the molecule. We note that there has been considerable improvement relative to the comparison of Fig.
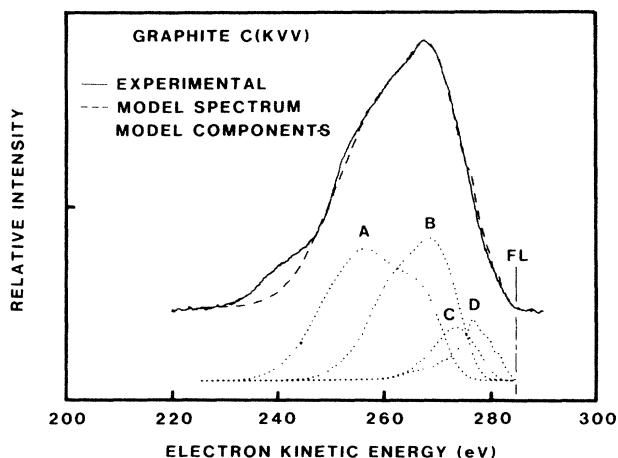

FIG. 8. A comparison of the experimental Auger line shape of POCO graphite (solid curve) with a model (dashed curve) which includes initial-state screening [with occupancy values calculated by Binkley (Ref. 50)], the Fermi-level valence-core excitonic state and the hole-hole interaction distortion calculated through the use of the Cini expression (Ref. 35). The components A, B, C, and D which sum to the model spectrum are, respectively, the $\sigma * \sigma$, $\sigma * \pi$, $\pi * \pi$, and the $(\sigma + \pi) *$ valence-core exciton (Ref. 57) contributions.

5 in the threshold region and in the area of the principal maximum. However, significant discrepancies remain in the region below 245 eV.

The general criterion for atomic localization obtained from the Cini-Sawatzky approach for single metallic bands depends on the relative magnitude of the bandwidth W compared to the value of U_{eff}. Here W refers to the total bandwidth (bonding plus antibonding) and is a measure of the strength of the covalent interaction. For $U_{eff} \ll W$ the final states are delocalized while for $U_{eff} \gg W$ the final states are strongly localized. Similar conclusions have been reached for covalent systems in terms of atomic, bonding, and group orbital contributions by Dunlap et al.[64]

The empirical values of U_{eff} obtained for the self-folds from the model fit in Fig. 8 appear to be reasonable based on a recent application of these criteria to graphite.[60] The screening in graphite would certainly be expected to result largely from $\pi - \pi^*$ mixing and this screening would be most effective for π-band holes. As mentioned, structure in the low-energy region of the line shape, where no intensity is expected on the basis of the one-electron model, could presumably be obtained by simply increasing the value of U_{eff} to the extent of creating a discrete state below the main portion of the line. However, estimates of U_{eff} from LCAO-ZDO (ZDO indicates zero differential overlap) calculations using various models for the effect of screening on U_{eff}, suggest that values for U_{eff} are not sufficient to give rise to strong localization. Thus, the broad feature in Fig. 8 centered at about 240 eV must be due to effects other than hole-hole localization.

4. Dynamic final-state screening

In the present section we briefly outline the effects on the Auger line shape of the dynamic aspects of final-state screening. Auger transitions which themselves leave the system in an excited state will produce structure at energies below that expected from the one-electron picture. These result from the so-called "shake" phenomena in the final state. Cini and D'Andrea[65] have recently discussed the effects of dynamic screening of the hole-hole interaction which can also lead to structure below that expected from the one-electron model.

The structure near 240 eV may indicate that dynamic final-state screening is contributing appreciably to the overall line shape. The Auger transition proceeds from a screened core-hole state to that of a neutral core and a two-hole state in the valence levels. From the standpoint of the core state, this transition is just the reverse of the core-excitation process and should give rise to the same array of dynamic screening features seen in the initial state.

The screening associated with the creation of a core hole in graphite has been extensively studied by a number of experimental techniques. Core-level XPS show characteristic loss structure associated with plasmon excitation[39] very similar to that shown in the backscatter spectrum of Fig. 1(e). These techniques, however, yield information regarding the extrinsic loss processes as well as the intrinsic dynamic screening processes and it is difficult to del-

ineate the contribution of the latter with reliable accuracy.[66,67]

Clear evidence for the intrinsic processes in graphite has been obtained from XES where there are no transport electrons to cause extrinsic loss processes.[68] Furthermore, core-level XPS for gas-phase benzene, where extrinsic loss processes should be greatly suppressed, show loss structure very similar to that of graphite.[69–71]

The dynamic aspects of the response to the creation of the initial-state core hole consist of a narrow excitation at a loss energy of about 7 eV [associated with the creation of a plasmon involving the $\pi-\pi^*$ states[72]], a broad excitation centered at a loss energy of approximately 27 eV (attributed to a plasmon creation involving a combination of σ, π, and σ^* states[72]), a broad featureless tail related to interband transitions, and a distortion of the symmetry of the core-level photoemission line associated with shakeup into the core-excitonic state.[56] With the exception of the core-excitonic state, all of these characteristics of the core-hole screening processes (including conduction-valence-band electron-hole creation) can be seen in the backscatter loss data for graphite shown in Fig. 1(e), which is very similar in shape to the core-level photoemission line for graphite.[39] Apparently only the valence-core excitonic shakeup in the initial state is sufficiently long-lived to significantly participate in the Auger decay. It is important to realize, however, that this lifetime effect is not important in the final state, and all of the final state dynamic screening excitations could possibly produce Auger intensity in the low-energy region of the line shape.

The position of the structure centered at about 240 eV in Fig. 8 is very near that expected to result from the 27 eV plasmon satellite of the Auger line itself. Indeed, much of the intensity in this region (the extrinsic portion) in the raw data of Fig. 1(a) was removed by the loss-deconvolution procedure. However, in the intrinsic plasmon emission process the satellite line would be expected to be broader than the Auger line itself, i.e., it would be characterized by the convolution of loss structure of Fig. 1(e) with the true Auger line shape.[73,74]

The width of the 240 eV feature can be estimated by assuming that the true Auger line shape is well represented by the model spectrum of Fig. 8 and subtracting it from the experimental line shape. The result of this procedure is shown in Fig. 9 where it is apparent that the width of the 240 eV feature is much narrower than that of the Auger line. Thus, it is unlikely that this feature can be identified as a normal intrinsic plasmon satellite, i.e., as a result of core-hole filling.

An alternate interpretation is suggested by the recent work of Cini and D'Andrea on the dynamical aspects of screening in determining Auger line shapes in solids.[65] In this work, dynamical effects (restricted to plasmon emission) are included by considering a plasmon field coupled to the two final-state holes interacting through the bare (unscreened) hole-hole repulsion, i.e., the inclusion of plasmon emission intrinsic to the two-hole final state rather than the core hole. The physical picture of the process is that the Auger final-state holes can be created with essentially a *bare hole-hole repulsion* and subsequently become delocalized through the emission of a plasmon.
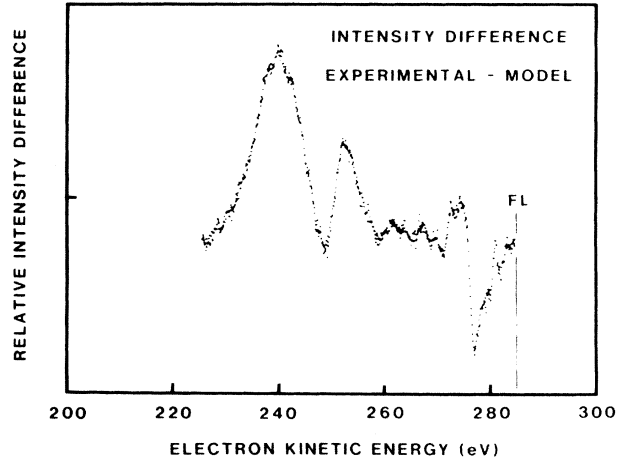

FIG. 9. The difference spectrum resulting from the subtraction of the model spectrum from the experimental Auger line shape of Fig. 8. The features located near 240 and 255 eV both appear considerably narrower than the Auger line shape itself.

Cini and D'Andrea[65] find that this new channel for the decay of the localized holes gives rise to several effects: (1) It can result in plasmon satellites in a case like graphite where the spectrum is distorted but still "band-like," (2) it can produce broadened but characteristic features within the "one-electron" line shape if the hole-hole distortion is strong but not discrete, and (3) it can produce a broadening of discrete or atomiclike features. In addition, it was found for case (1) that the shape of the plasmon satellite did not reflect the shape of the principal Auger structure. In fact, for an assumed square model DOS, Cini and D'Andrea[65] find a plasmon satellite that is a broad shoulder reminiscent of the 240 eV feature in our graphite results shown in Fig. 2. This type of phenomenon seems a likely candidate to account for the remaining discrepancies between our model and the experimental data shown in Fig. 8.

V. SUMMARY AND CONCLUSIONS

We have obtained the Auger spectrum for POCO graphite from data taken in two separate laboratories and on three different types of electron-energy analyzers. These separate data were independently corrected for the effects of secondary-electron background and extrinsic losses. In addition, considerable care was taken to ensure that the absolute energy scale was accurate. The result is a graphite Auger line shape which we feel is as free as possible from experimental and data-reduction artifacts.

In characterizing the Auger structure in terms of the one-electron approximation with atomic Auger matrix elements, we find a model line shape which differs considerably from that of the experiment. Intensity is missing in the model function at both the high- and low-energy ends of the spectrum and there are significant differences in relative intensity throughout the main body of the line.

To characterize the discrepancies seen between the ex-

perimental line shape and the one-electron Auger model, we have considered both the static and dynamic aspects of initial- and final-state screening. We find that the static polarization effect of initial-state screening has a negligible influence on the line shape. However, valence electron shakeup into the core-excitonic level places charge in an energy region where very little exists in ground-state graphite giving rise to significant new intensity in the Auger line shape just below the threshold level. Modeling the dynamic Auger effect by the inclusion of a delta-function density of states at the threshold energy and assuming that the valence-core excitonic electron participates in the Auger process along with a valence electron, results in a dramatic improvement between the measured and model line shapes in the high-energy region for an effective electron occupancy in this excited state of 0.27.

The distorting effect on the predicted line shape resulting from the hole-hole interaction in the Auger final state has been modeled using the Cini expression.[35,36] We have assumed that the empty portions of the σ and π bands are separated sufficiently from each other and from the filled portions to permit the use of the Cini filled-band formal-

ism by including screened hole-hole repulsion parameters for the $\sigma*\sigma$, $\sigma*\pi$, and $\pi*\pi$ contributions. Under these assumptions, the application of the Cini expression results in considerable improvement of the model line shape in the region below the principal maximum.

The final area of disagreement in the model line shape consists of a shoulderlike feature on the low-energy side of the Auger line which is not accounted for by localization effects. We suggest, on the basis of more recent work by Cini,[65] that this structure is due to a plasmon effect intrinsic to the two-hole final state in the Auger process. The adequate characterization of this feature will undoubtedly require a theoretical model which includes multiple, partially-filled bands with the inclusion of dynamical final-state effects.

ACKNOWLEDGMENTS

[1]P. H. Holloway, Adv. Electron. Electron Phys. **54**, 241 (1980).

[2]F. Netzer, Appl. Surf. Sci. **7**, 289 (1981).

[3]P. Weightman, Rep. Prog. Phys. **45**, 753 (1982).

[4]G. G. Kleiman, Appl. Surf. Sci. **11 & 12**, 730 (1982).

[5]F. P. Larkins, Appl. Surf. Sci. **13**, 4 (1982).

[6]H. H. Madden, J. Vac. Sci. Technol. **18**, 677 (1981).

[7]J. C. Fuggle, in *Electron Spectroscopy: Theory, Technique and Applications*, edited by C. R. Brundle and A. D. Baker (Academic, New York, 1981), Vol. 4, pp. 85–149.

[8]D. E. Ramaker, *Chemistry and Physics of Solid Surfaces IV*, edited by R. Vanselow and R. Howe (Springer-Verlag, Heidelberg, 1982), p. 19.

[9]D. R. Jennison, J. Vac. Sci. Technol. **20**, 548 (1982).

[10]R. R. Rye and J. E. Houston, Acc. Chem. Res. **17**, 41 (1984).

[11]R. Weissmann and K. Muller, Surf. Sci. Rep. **105**, 251 (1981).

[12]J. A. D. Matthew, Phys. Scr. **T6**, 79 (1983).

[13]J. T. Grant, Appl. Surf. Sci. **13**, 35 (1982).

[14]H. Agren, J. Chem. Phys. **75**, 1267 (1981).

[15]P. Weightman, Rep. Prog. Phys. **45**, 753 (1982).

[16]S. I. J. Ingrey, Can. J. Spectrosc. **28**, 73 (1983).

[17]L. L. Levenson, Scanning Electron Microsc. **IV**, 1643 (1983).

[18]J. C. Riviere, United Kingdom Atomic Energy Research Establishment (Oxfordshire, England), Harwell Report No. 10384, 1982 (unpublished).

[19]D. E. Ramaker, Appl. Surf. Sci. **21**, 243 (1985).

[20]M. Thompson, M. D. Baker, A. Christie, and J. F. Tyson, *Auger Electron Spectroscopy*, Vol. 74 of *Chemical Analysis* (Wiley, New York, 1985).

[21]J. S. Murday, B. I. Dunlap, F. L. Hutson, II, and P. Oelhafen, Phys. Rev. B **24**, 4764 (1981).

[22]S. D. Bader, Solid State Commun. **35**, 501 (1980).

[23]M. A. Smith and L. L. Levenson, Phys. Rev. B **16**, 2973 (1977).

[24]J. A. Tagle, V. Marinez Saez, J. M. Rojo, and M. Salmeron, Surf. Sci. **79**, 77 (1978).

[25]G. F. Amelio and E. J. Scheibner, Surf. Sci. **11**, 242 (1968).

[26]B. I. Dunlap, D. E. Ramaker, and J. S. Murday, Phys. Rev. B

25, 6439 (1982).

[27]D. Marchand, C. Fretigny, M. Lagues, and P. Lagrand, Synth. Met. **8**, 125 (1983).

[28]P. Oelhafen, P. Pfluger, E. Hauser, and H. J. Guntherodt, Phys. Rev. Lett. **44**, 197 (1980).

[29]P. Oelhafen, P. Pfluger, and H. J. Guntherodt, Solid State Commun. **32**, 885 (1979).

[30]D. R. Jennison, Phys. Rev. A **23**, 1215 (1981).

[31]J. E. Houston, in *Methods of Surface Characterization*, edited by C. J. Powell, T. E. Madey, J. T. Yates, A. W. Czanderna, and D. M. Hercules (Plenum, New York, in press), Vol. 1.

[32]E. N. Sickafus, Rev. Sci. Instrum. **42**, 933 (1971).

[33]E. N. Sickafus, Phys. Rev. B **16**, 1436 (1977).

[34]E. N. Sickafus, Phys. Rev. B **16**, 1448 (1977).

[35]M. Cini, Solid State Commun. **20**, 605 (1976).

[36]M. Cini, Phys. Rev. B **17**, 2788 (1978).

[37]G. A. Sawatzky, Phys. Rev. Lett. **39**, 504 (1977).

[38]H. H. Madden and J. E. Houston, J. Appl. Phys. **47**, 3071 (1976).

[39]F. R. McFeely, S. P. Kowalczyk, L. Ley, R. G. Cavell, R. A. Pollak, and D. A. Shirley, Phys. Rev. B **9**, 5268 (1974).

[40]J. W. Rogers, Jr., R. R. Rye, and J. E. Houston (unpublished).

[41]Ch. Beyreuther and G. Wiech, Phys. Fenn. **9**, 176 (1974).

[42]R. F. Willis, B. Fitton, and G. S. Painter, Phys. Rev. B **9**, 1926 (1974).

[43]G. S. Painter and D. E. Ellis, Phys. Rev. B **1**, 4747 (1970).

[44]R. C. Tatar and S. Rabii, Phys. Rev. B **25**, 4126 (1982).

[45]J. E. Holliday, in *Soft X-ray Band Spectra and the Bond Structure of Metals and Materials*, edited by D. J. Fabian (Acadencia, New York, 1968), p. 101.

[46]H. P. Kelly, Phys. Rev. A **11**, 556 (1975).

[47]D. E. Ramaker, Phys. Rev. B **25**, 7341 (1982).

[48]G. A. Sawatzky, J. Solid State Chem. **3**, 3 (1982).

[49]D. E. Ramaker, F. L. Hutson, N. Turner, and W. N. Mei, Phys. Rev. B **33**, 2574 (1986).

[50]J. S. Binkley (unpublished).

[51]W. E. Moddeman, T. A. Carlson, M. O. Krause, B. P. Pullen,

W. E. Bull, and G. K. Schweitzer, J. Chem. Phys. **50**, 2317 (1971).

[52]S. D. Bader, G. Zajac, and J. Zak, Phys. Rev. Lett. **50**, 1211 (1983); G. Zajac, S. D. Bader, and J. Zak, J. Vac. Sci. Technol. A **2**, 933 (1984).

[53]E. Bertel, R. Stockbauer, and T. E. Madey, Surf. Sci. **141**, 355 (1984).

[54]E. J. Mele and J. J. Ritsko, Phys. Rev. Lett. **43**, 68 (1979).

[55]E. J. McGuire, Phys. Rev. A **2**, 273 (1970); Phys. Rev. **185**, 1 (1969).

[56]P. M. Th. M. van Attekum and G. K. Wertheim, Phys. Rev. Lett. **43**, 1896 (1979).

[57]J. E. Houston, D. E. Ramaker, J. W. Rogers, Jr., R. R. Rye, and F. L. Hutson, Phys. Rev. Lett. **56**, 1302 (1986).

[58]M. Cini, Surf. Sci. **87**, 483 (1979).

[59]V. Drchal and J. Kudrnovsky, J. Phys. F **14**, 2443 (1984).

[60]D. E. Ramaker, F. L. Hutson, R. R. Rye, J. E. Houston, and J. W. Rogers, Jr., J. Vac. Sci. Technol. A **2**, 1146 (1984).

[61]P. Weightman and P. T. Andrews, J. Phys. C **13**, 3529 (1980).

[62]P. Weightman and P. T. Andrews, J. Phys. C **13**, 815 (1980).

[63]D. E. Ramaker, Phys. Rev. B **21**, 4608 (1980).

[64]B. I. Dunlap, F. Hutson, and D. E. Ramaker, J. Vac. Sci. Technol. **18**, 556 (1981).

[65]M. Cini and A. D'Andrea, Phys. Rev. B **29**, 6540 (1984).

[66]A. M. Bradshaw, W. Domcke, and L. S. Cederbaum, Phys. Rev. B **16**, 1480 (1977).

[67]J. C. Fuggle, D. J. Fabian, and L. M. Watson, J. Electron. Spectrosc. Relat. Phenom. **9**, 99 (1976).

[68]O. Aita, I. Nagakura, and T. Sagawa, J. Phys. Soc. Jpn. **30**, 516 (1971).

[69]S. Lunell, S. Svensson, P. A. Malmqvist, U. Gelius, E. Basilier, and K. Siegbahn, Chem. Phys. Lett. **54**, 420 (1978).

[70]J. Riga, J. J. Pireaux, and J. J. Verbist, Mol. Phys. **34**, 131 (1977).

[71]R. M. Bigelow and H. J. Freund, J. Chem. Phys. **77**, 5552 (1982).

[72]K. Zeppenfeld, Phys. Lett. **25A**, 335 (1967).

[73]A. L. Hagen and A. J. Glick, Phys. Rev. B **13**, 1580 (1976).

[74]G. A. Rooke, Phys. Lett. **3**, 234 (1963).